Deconvolution Analysis of Ga K-Edge XANES for Quantification of Gallium Coordinations in Oxide Environments

Koji Nishi,*,†,‡ Ken-ichi Shimizu,‡ Mikio Takamatsu,‡ Hisao Yoshida,*,‡ Atsushi Satsuma,‡ Tsunehiro Tanaka,§ Satohiro Yoshida,§ and Tadashi Hattori||

Department of Applied Chemistry, Graduate School of Engineering, Nagoya University, Chikusa-ku, Nagoya 464-8603, Japan, Department of Molecular Engineering, Graduate School of Engineering, Kyoto University, Sakyo-ku, Kyoto 606-8501, Japan, Research Center for Advanced Waste and Emission Management, Nagoya University, Chikusa-ku, Nagoya 464-8603, Japan

Received: June 22, 1998; In Final Form: August 29, 1998

A quantitative analysis of gallium species (GaO_4 tetrahedra and GaO_6 octahedra) by means of X-ray absorption spectroscopy (XANES and EXAFS) at the Ga K-edge was performed on a series of gallium oxides with various phases and SiO_2-supported ones. XANES spectra of gallium oxides showed two distinguishable peaks that were assigned to tetrahedral and octahedral gallium oxide species on the basis of a comparison with those of reference compounds. A deconvolution analysis of XANES spectra was carried out on the assumption that the absorption due to each species is expressed by a set of Gaussian and arctangent functions, and the tetrahedral/octahedral ratios were quantitatively estimated from the ratio of the peak areas. By the EXAFS curve-fitting analysis, the tetrahedral/octahedral ratios were also estimated, and they were in good agreement with those obtained by XANES analysis. It was concluded that the Ga atoms with a different coordination symmetry (tetrahedral or octahedral) can be estimated quantitatively by a deconvolution analysis of XANES.

Introduction

Gallium-containing catalysts have become of great interest. For example, gallium-promoted zeolites are used for the transformation of lower alkanes into aromatic hydrocarbons and dehydrogenation or oxidehydrogenation of lower alkanes.[1−4] It is well-known that these catalysts contain gallium oxide, which is present as small particles, and this phase itself exhibits catalytic activity for alkane dehydrogenation.[1,2,4] However, the structure of such gallium species is still unclear because of difficulties in its structural analysis.

Gallium oxides catalysts, which are normally calcined at temperatures at ca. 700−1000 K, can include various transitional phases,[5] as in the case of alumina.[6] Some of them have well-known structures; the β phase has a spinel structure, containing both tetrahedral and octahedral Ga ions,[7] whereas the α phase has a corundum structure, containing only octahedral Ga ions.[8] However, the structure of other gallium oxides, such as ϵ, γ, and ∂ phases, are not precisely known because of their poor crystallinity.[5] For the aluminas, for which it is also difficult to determine the precise structure,[6] ^{27}Al MAS NMR was successfully used to distinguish several Al atoms with different local structures.[9,10] However, application of ^{69}Ga and ^{71}Ga MAS NMR to the quantitative analysis is difficult because of the line broadening caused by strong quadrupolar interactions of Ga atoms.[11−14]

X-ray absorption spectroscopy (EXAFS/XANES) is another tool for investigating the local structures.[15,16] EXAFS, in particular, is known to give structural data quantitatively, although its analysis requires a lot of care to draw a meaningful conclusion. In contrast, XANES is rather unpopular as a tool for quantitative analysis, since its theoretical interpretation is complicated as a result of the complexity of the phenomena. Although the fine structure observed above the edge, so-called white line, can reflect the local site symmetry around the X-ray absorbing atom, analysis of this region is mainly still of a fingerprint. For example, in our recent study by Ga L_3-edge XANES, gallium oxides dispersed on the SiO_2 and Al_2O_3 support were shown to have specific local structures,[17] but the detailed microstructure of the gallium species remains unclear. In the present study, we demonstrate that the Ga atoms with different coordination symmetry can be estimated quantitatively for supported and unsupported Ga_2O_3 samples by the deconvolution analysis of Ga K-edge XANES, and the validity of the analysis is confirmed by comparison with the EXAFS data of the same samples.

Experimental Section

A series of unsupported and supported Ga_2O_3 samples, listed in sections a and b of Table 1, respectively, were prepared in various ways to obtain a wide structural variety of Ga_2O_3. β-Ga_2O_3 (N-6) was purchased from Mitsuwa Chemicals. Other unsupported Ga_2O_3 samples were prepared by calcining gallium hydroxide (H-*n*) or gallium nitrate (N-*n*) at various temperatures in a dry air stream. SiO_2-supported Ga_2O_3 samples (S-*n*) were prepared by impregnation of SiO_2 (reference catalyst,[18] Catalysis Society of Japan, JRC-SIO-8, BET surface area 303 m^2/g) with an aqueous solution of gallium nitrate followed by evaporation to dryness and calcination in air at 823 K for 4 h. $Ga(acac)_3$ was purchased from Aldrich. MFI-type gallosilicate zeolite (Ga-MFI) containing a small amount of Ga (Si/Ga = 80) in the framework was synthesized hydrothermally and calcined at 823

* To whom correspondence should be addressed.
† Present address: Department of Chemistry, National Defense Academy, Hashirimizu, Yokosuka 239-8686, Japan.
‡ Department of Applied Chemistry, Nagoya University.
§ Department of Molecular Engineering, Kyoto University.
|| Research Center for Advanced Waste and Emission Management, Nagoya University.

10.1021/jp982704p CCC: $15.00
Published on Web 11/19/1998

TABLE 1: List of Ga_2O_3 Samples

Unsupported Ga_2O_3

sample	precursor	calcination temp/K	calcination time/h	crystal phase (XRD)	particle size/nm (BET)
H-1	*a*	823	2	α, ϵ	8.92
H-2	*b*	823	6	α, (ϵ)	19.6
H-3	*b*	923	4	α, (ϵ)	25.8
H-4	*c*	823	4	α, (ϵ)	68.2
H-5	*b*	1073	4	β	41.7
N-1	*d*	823	2	ϵ, γ	13.5
N-2	*d*	823	4	ϵ	14.3
N-3	*d*	923	4	β	18.4
N-4	*d*	1073	4	β	44.1
N-5	*d*	1073	4	β	27.8
N-6	*e*			β	240

Supported Ga_2O_3

sample	Ga_2O_3 content/wt %	crystal phase (XRD)	particle size/nm (TEM)
S-1	4.0	amorphous	2.0
S-2	6.7	amorphous	2.4
S-3	13	(ϵ)	3.2
S-4	27	(ϵ)	6.2

[a] Gallium hydroxide prepared by adding the mixture of dodecyltrimethylammonium bromide and gallium nitrate solution to ammonia solution of pH = 9.0 at 343 K. [b] Commercially supplied gallium hydroxide (Mitsuwa Chemicals). [c] Gallium hydroxide prepared by adding ammonia solution of pH = 8.5 to gallium nitrate solution at 343 K followed by aging overnight. [d] Commercially supplied gallium nitrate (Mitsuwa Chemicals). [e] Commercially supplied β-Ga_2O_3 (Mitsuwa Chemicals).

K for 4 h. The purity of the MFI-type structure was confirmed by XRD.

The X-ray diffraction pattern of the powdered catalysts was recorded with a Rigaku RINT 1200 diffractometer. BET surface areas of the unsupported Ga_2O_3 samples were measured by using nitrogen adsorption at 77 K, and the particle size of Ga_2O_3 was estimated from the surface area by assuming that the shape of the particle is a sphere. The particle size of SiO_2-supported Ga_2O_3 was estimated by transmission electron microscopy (TEM, JEOLJEM-2010).

Ga K-edge XAFS spectra were recorded at BL-10B[19] of Photon Factory in High Energy Accelerator Research Organization, Tsukuba, Japan, with a ring energy of 2.5 GeV and a stored current of 250−350 mA. The spectra were recorded in transmission mode at room temperature with a Si(311) channel-cut monochromator (d = 1.6375 Å). The intensities of the incident and transmitted X-rays were measured with a 17 cm ion chamber with a flowing gas mixture of N_2 (85%) and Ar (15%) and a 31 cm ion chamber with a flowing gas mixture of N_2 (75%) and Ar (25%), respectively. The estimated resolution was about 1 eV at around the Ga K-edge (10371 eV).[19] The data were collected with an energy step of ca. 0.5 eV at 10371 eV. Normalization of XANES and data reduction on EXAFS were carried out as described elsewhere.[20] For curve-fitting analysis, the following equation was applied.

$$k^3\chi = k^2\sum\frac{A_j(k)N_j}{R_j}2[\exp(-2\Delta\sigma_j{}^2k^2)]\sin(2kR_j + \delta_j(k))$$

where k is the wavenumber of the photoelectron, N_j the number of scattering atoms of the jth shell located at a distance of R_j from a gallium atom, A_j the envelope function that includes the backscattering amplitude and damping factor caused by inelastic loss during the electron traveling, $\Delta\sigma_j$ the Debye−Waller factor, and δ_j the phase shift. Fourier filtering was performed typically between 1.0 and 2.0 Å. A_j and δ_j were extracted from Ga(acac)$_3$, and hence, $\Delta\sigma_j$ corresponds to the relative Debye−Waller factor that deviated from that of the compound. The average Ga−O distance in Ga(acac)$_3$, 1.952 Å,[21] was employed as a standard of distance.

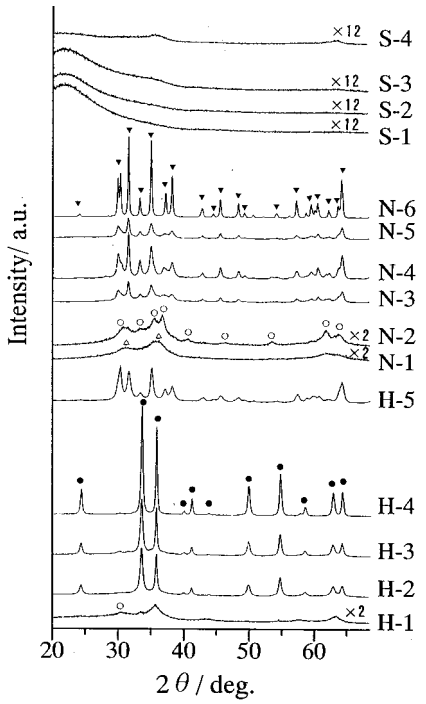

Figure 1. XRD pattern of the gallium oxide samples: ●, α-Ga_2O_3; ▼, β-Ga_2O_3; ○, ϵ-Ga_2O_3; △, γ-Ga_2O_3.

Results and Discussion

Conventional Characterization. Table 1 summarizes the results of the conventional characterization. The crystal phase was confirmed by the XRD pattern shown in Figure 1. When the preparation method was changed, a series of gallium oxide samples were obtained as follows. Commercially supplied gallium oxide, N-6, exhibited the β phase with high crystallinity. The samples prepared by calcining gallium nitrate above 923 K (N-3,4,5) and that prepared by calcining gallium hydroxide at 1073 K (H-5) exhibited broader diffraction lines due to the β phase, indicating the poorer crystallinity of the samples. The samples prepared by calcining gallium nitrate at 823 K showed the ϵ phase (N-2) or the mixture of ϵ and γ phases (N-1). The samples prepared by calcining gallium hydroxide below 923 K (H-1,2,3,4) exhibited diffraction lines due to the α phase and a very weak line at around 30.5° possibly due to phase, the latter of which is appreciable for the H-1 sample. Among these samples, H-4 exhibited the highest crystallinity of α phase. For SiO_2-supported samples, no lines due to gallium oxides were observed for the samples below 6.7 wt % (S-1,2). For the samples above 13 wt % (S-3,4), very broad lines probably due to the ϵ phase were observed but could not be identified clearly. The particle size changed from 2.0 to 6.2 nm as the Ga_2O_3 content increases. Thus, a series of gallium oxides with a variety of crystal phases, crystallinity, and particle sizes (2.0−240 nm) were obtained.

Ga K-Edge XANES. Ga K-edge XANES spectra for the samples are shown in Figure 2 together with those of some reference compounds of known structure. As a reference

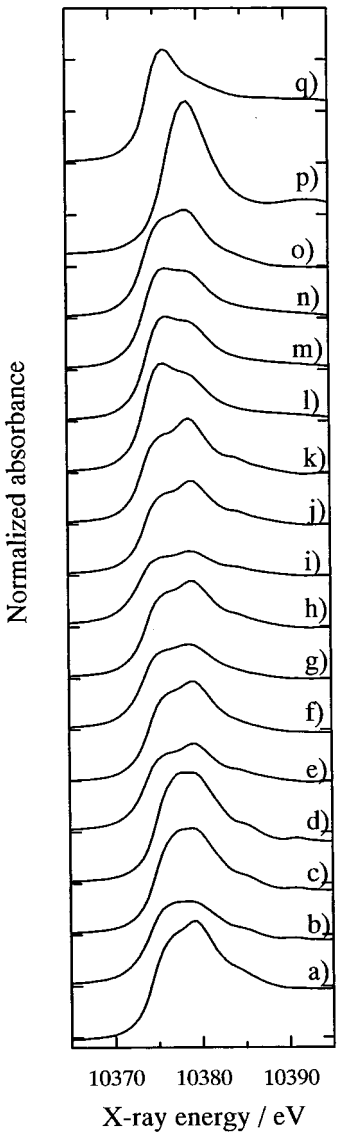

Figure 2. Ga K-edge XANES spectra of supported and unsupported Ga_2O_3 samples and reference samples: (a) H-1, (b) H-2, (c) H-3, (d) H-4, (e) H-5, (f) N-1, (g) N-2, (h) N-3, (i) N-4, (j) N-5, (k) N-6, (l) S-1, (m) S-2, (n) S-3 (o) S-4, (p) $Ga(acac)_3$, and (q) MFI-type gallosilicate.

compound for octahedral Ga^{3+} species, $Ga(acac)_3$ was employed, since the six oxygen atoms form a nearly ideal octahedron.[21] The XANES spectrum of $Ga(acac)_3$ (Figure 2p) exhibited a rather symmetric and narrow peak at 10379 eV, which is due to the 1s → 4p electron transition.[22] The peak at 10379 eV will be assigned to the octahedral Ga species, which will be referred to as Ga(o) hereafter. Ga-MFI was used as a reference compound for the tetrahedral Ga^{3+} species. Tetrahedral coordination of Ga was confirmed by MAS NMR. The XANES spectrum of Ga-MFI (Figure 2q) exhibited a peak at 10375 eV, which will be assigned to the tetrahedral Ga species, which will be referred to as Ga(t). In comparison with the spectrum of $Ga(acac)_3$, the peak position of the spectrum of Ga-MFI appeared at lower energy. In addition, the white line intensity of Ga-MFI was smaller than that of $Ga(acac)_3$. It should be noted that the symmetry of Ga in the MFI-type zeolite framework slightly deviates from an ideal tetrahedron; a density functional study[23] has shown that the average of the three O−Ga−O angles is 106.5°, while the average of the other three O−Ga−O angles is 112.5°, which are different from that of ideal tetrahedral geometry, 109.5°. This would result in a rather small intensity of the white line of Ga-MFI.

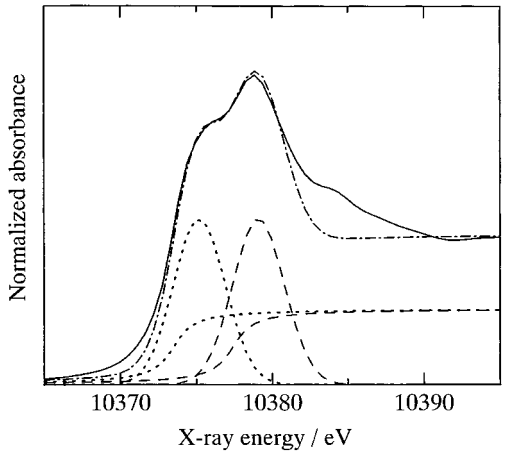

Figure 3. Ga K-edge XANES of β-Ga_2O_3 (N-6, solid line) and the simulated spectrum (-•-), which is composed of two sets of Gaussian and arctangent functions (dotted and broken).

Recently, Wong et al.[24] reported that the Al K-edge peak was shifted to a higher energy with an increase of the oxygen coordination number of Al from 4 to 6 (sodalite to kyanite). They also recorded Si K-edge XANES of Si, SiC, Si_3N_4 and SiO_2 and showed that the Si K-edge shifted to the high-energy side with an increase of electronegativity of the nearest-neighbor ligand. They explained that the binding energy of the 1s electron, and hence the edge energy, is progressively increased as a result of the increased effective nuclear charge caused by a decrease in the screening of the nucleus by the valence electrons. It is known for some transition metal systems that the edge energy is increased as the valence (cation charge) of the metal is increased.[15,25−28] For manganese oxides, the edge energy shifts when going from the Mn metal through MnO(II) and MnO_2(IV) to MnO_4^-(VII) are 5.6, 13.3, and 19.1 eV, respectively.[25] It should be noted that the observed energy shift of the Ga K-edge white line, 4 eV, is relatively small with respect to that due to the valence state change of metal ion. From the above-mentioned discussion, it is considered that the positive shift of the Ga K-edge peak energy can be due to an increase of the electronegativity of the nearest-neighbor ligand of Ga^{3+} ion with an increase of oxygen coordination number of Ga.

Figure 2 includes the Ga K-edge XANES of unsupported and supported gallium oxide samples. For commercially available β-Ga_2O_3 (N-6, Figure 2k), in which Ga atoms are equally distributed between the tetrahedral and octahedral site of the spinel,[7] the XANES spectrum exhibited an absorption maximum at 10375 eV and a shoulder at about 10379 eV, which were assigned above to Ga(t) and Ga(o), respectively. In addition, a small peak at 10385 eV is observed. Since the last peak appears in the postedge region, which is influenced by a multiple scattering of photoelectrons by neighboring atoms,[16] it was not employed for the analysis in the present study. For unsupported Ga_2O_3 samples prepared from either hydroxide (Figure 2a−e) or nitrate (Figure 2f−j) and for the SiO_2-supported Ga_2O_3 samples (Figure 2l−o), XANES spectra contain both peaks at 10 379 and 10 375 eV with different relative intensities. It is likely that the samples contain two kinds of Ga species, Ga(t) and Ga(o), and the fraction of each species differs from sample to sample.

Deconvolution Analysis of XANES. To estimate the ratio of Ga(t)/Ga(o) quantitatively, the deconvolution analysis of

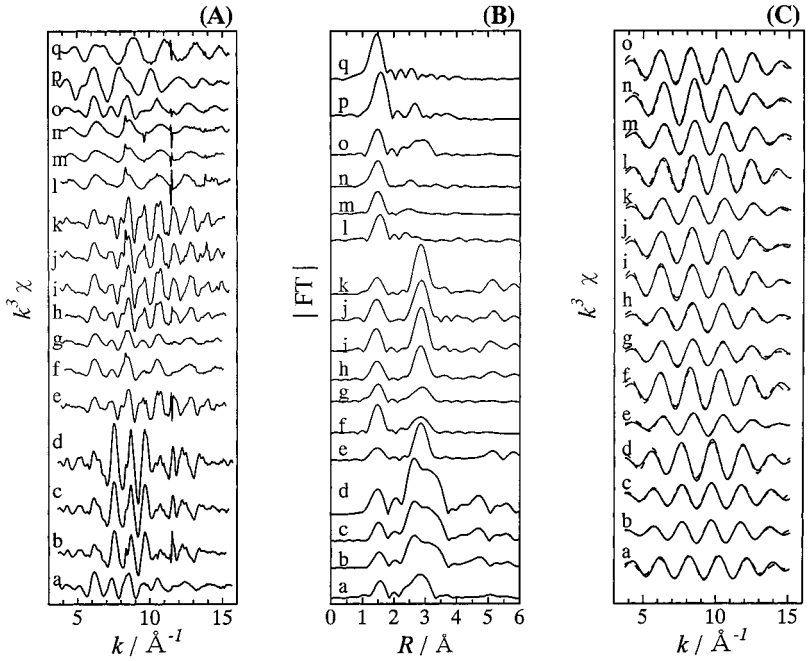

Figure 4. Ga K-edge EXAFS of gallium oxides: (A) $k^3\chi(k)$ data; (B) radial structural function derived from Fourier transform of data shown in (A), not corrected for phase shift; (C) Fourier filtered EXAFS function of the first shell (solid line) and resulting curve fit (dotted line) used to calculate structural parameters. Samples a−q are the same as in Figure 2.

TABLE 2: Parameters of Deconvoluted Peaks in XANES Spectra of Gallium Oxide

	Ga(t) species/eV			Ga(o) species/eV			
sample	position	fwhm	area	position	fwhm	area	Ga(t)/Ga(o)
H-1	10 375.2	3.5	3.0	10 379.2	5.5	6.2	0.48
H-2	10 375.1	4.0	3.0	10 379.2	6.2	4.6	0.65
H-3	10 375.2	3.6	2.4	10 379.0	6.2	6.4	0.38
H-4	10 375.2	3.5	1.7	10 378.8	6.6	7.4	0.23
H-5	10 375.2	4.1	3.5	10 379.3	5.0	4.1	0.85
N-1	10 375.2	3.6	3.1	10 379.1	5.3	5.1	0.61
N-2	10 374.7	4.0	3.0	10 378.9	6.1	4.7	0.64
N-3	10 375.2	3.8	3.7	10 379.2	5.1	5.2	0.71
N-4	10 375.2	3.8	3.6	10 379.3	4.5	4.6	0.78
N-5	10 375.2	4.0	3.2	10 379.1	4.5	3.7	0.86
N-6	10 375.2	4.0	4.7	10 379.1	4.0	4.7	1.0
S-1	10 375.5	4.2	6.4	10 379.3	4.0	3.5	1.8
S-2	10 375.6	4.1	5.9	10 379.4	4.1	3.6	1.6
S-3	10 375.5	4.2	5.8	10 379.3	4.1	3.7	1.6
S-4	10 375.3	3.8	4.5	10 379.0	4.8	5.5	0.82

XANES spectra was carried out following the method in the previous study.[16,29] Figure 3 illustrates a deconvoluted spectrum of β-Ga_2O_3 (N-6) as an example. The simulation of the spectrum was made on the basis of the following assumptions:[1] the spectrum is composed of two components;[2] each component consists of an arctangent curve for continuum absorption and a Gaussian curve for the white line;[3] the energy of the inflection point of arctangent curve is the same as that of corresponding Gaussian curve;[4] the ratio of the height of each arctangent curve is equal to the ratio of the peak area of each Gaussian curve. Thus, the best parameters, i.e., the exact peak energy, the fwhm, and the peak area of each Gaussian were determined to simulate the original spectra and were listed in Table 2. For β-Ga_2O_3 (N-6), the positions of two Gaussian peaks were determined to be 10 375.2 and 10 379.1 eV, which were almost identical to those of Ga(t) and Ga(o), respectively. In addition, the ratio of the integrated intensities of these peaks was calculated to be 1.0, which is in good agreement with the Ga(t)/Ga(o) ratio in the literature.[7] These results suggest that the ratio of Ga(t)/Ga(o) in the gallium oxide can be estimated quantitatively by this method. Table 2 summarizes the best-fitting parameters of the samples. The positions of two Gaussian peaks were centered at 10 375.20 ± 5 and 10 379.10 ± 7 eV, which were almost identical to those of Ga(t) and Ga(o), respectively, within experimental error. It was considered that the Ga(t)/Ga(o) ratio can be estimated from the ratio of each Gaussian peak areas. The validity of this analysis for a series of samples will be confirmed by comparison with the EXAFS data in the following section.

As shown in Table 2, the Ga(t)/Ga(o) ratio varied with preparation procedure. For the samples exhibiting XRD lines of β-Ga_2O_3 (H-5, N-3,4,5,6), the Ga(t)/Ga(o) ratio was around 0.71−1.0. Deviations from the value of the ideal β phase (1.0) should be due to the lack of crystallinity of the samples. For H-2,3,4 samples, the Ga(t)/Ga(o) ratio was relatively low, which is consistent with the XRD result that these samples consist mainly of α-Ga_2O_3 containing only the octahedral Ga atoms. The Ga(t)/Ga(o) ratio was lowest for H-4 (0.23), which has the highest crystallinity of α-Ga_2O_3. Deviations from the ratio for the ideal α phase (0) should be due to the presence of the other phase, such as the ϵ phase, and/or a lack of crystallinity. For the SiO_2-supported samples having amorphous gallium oxide,

TABLE 3: Results of EXAFS Curve-Fitting Analyses of Gallium Oxide Samples

	Ga(t) species			Ga(o) species			
sample	N_t	R_t/Å	σ_t^2	N_o	R_o/Å	σ_o^2	Ga(t)/Ga(o)[a]
H-1	1.2	1.90	−0.003	4.7	2.00	0.073	0.36
H-2	0.33	1.82	−0.006	1.0	2.00	0.001	0.49
H-3	0.50	1.82	−0.006	2.6	1.99	0.011	0.28
H-4	1.1	1.81	−0.005	5.8	2.00	0.024	0.28
H-5	1.1	1.85	−0.002	2.1	1.99	0.003	0.83
N-1	1.8	1.88	−0.003	3.7	2.00	0.023	0.72
N-2	1.5	1.86	−0.002	3.2	2.00	0.040	0.70
N-3	1.2	1.86	−0.003	2.5	2.00	0.038	0.72
N-4	1.8	1.85	−0.002	2.9	2.00	0.012	0.95
N-5	1.8	1.86	−0.002	2.7	2.00	0.021	1.02
N-6	1.7	1.85	−0.001	2.7	2.00	0.029	0.92
	(2.0)[b]	(1.83)[b]		(3.0)[b]	(2.00)[b]		(1.00)[b]
S-1	1.7	1.87	−0.003	1.5	2.00	0.037	1.7
S-2	1.6	1.84	−0.003	1.6	2.00	0.029	1.5
S-3	2.8	1.85	−0.000	2.5	2.00	0.022	1.7
S-4	1.6	1.87	−0.004	2.7	2.00	0.010	0.89

[a] Ga(t)/Ga(o) ratio is calculated by the following equation: $(N_t/4)/(N_o/6)$. [b] Crystallographic data of β-Ga_2O_3.[25]

the Ga(t)/Ga(o) ratio is much larger than that of unsupported samples. The ratio was highest for the sample of the lowest content (S-1) having the smallest particle size (2 nm). This indicates that tetrahedral Ga species are predominant for highly dispersed gallium oxide on the SiO_2 support possibly because of a strong interaction with the SiO_2 matrix.

Ga K-Edge EXAFS. Figure 4A shows k^3-weighted Ga K-edge EXAFS spectra. The Fourier transform was performed on these EXAFS in the 3.8−15.1 $Å^{-1}$ region, and the radial structure function (RSF) was obtained as shown in Figure 4B. Peaks appearing at 1−2 Å are due to the backscattering from the adjacent oxygen atoms, and peaks at 2−3 Å show the presence of the second-neighboring metal atoms (Ga or Si atoms). The positions of the Ga−O shell of reference compounds are 1.45 for Ga-MFI and 1.65 for $Ga(acac)_3$, which agree with the fact that the average Ga−O distance of Ga-MFI, 1.78 Å,[23] is shorter than that of $Ga(acac)_3$, 1.95 Å.[21]

The inverse Fourier transform of the first Ga−O shell (R = 1−2 Å) in the RSF gives the EXAFS spectrum due to the Ga−O, as shown in Figure 4C with solid lines. Curve-fitting was performed in the k region of 3.8−15.1 $Å^{-1}$ with two Ga−O shells. As shown in Figure 4C, the simulated spectra (dotted lines) fit well with the experimental spectra. It should be noted that one-shell fitting resulted in poorer fits. The resulting structural parameters for Ga−O shell are given in Table 3. For the reference sample, β-Ga_2O_3 (N-6), the curve-fitting results indicate coordination shells with 1.7 oxygen atoms at 1.85 Å and 2.7 oxygen atoms at 2.00 Å, which is in good agreement with the crystallographic data. Thus, the reliability of the amplitude and the phase shift extracted from $Ga(acac)_3$ are confirmed. Taking into account the fact that the average bond distances for β-Ga_2O_3 are 1.83 Å for Ga(t)−O and 2.00 Å for Ga(o)−O,[7] we assumed the Ga−O shells with bond distances of 1.85 and 2.00 Å to be Ga(t)−O and Ga(o)−O, respectively. By use of the coordination numbers for each shell, N_t and N_o, the ratio of Ga(t) species to Ga(o) species, Ga(t)/Ga(o) = $(N_t/4)/(N_o/6)$, can be estimated and was included in Table 3. For the samples, the best fit parameters shown in Table 3 were obtained with two Ga−O shells with Ga−O distances of 1.86 ± 0.04 and 2.00 ± 0.01 Å, which were assumed to be Ga(t)−O and Ga(o)−O, respectively. The Ga(t)/Ga(o) ratios of the samples were also calculated from the coordination numbers and included in Table 3.

Validity of XANES Analysis. Figure 5 shows a plot of the Ga(t)/Ga(o) ratio in the samples derived from the deconvolution analysis of XANES versus that from the curve-fitting analysis of EXAFS. Clearly, proportional relationship is obtained with a slope of unity, indicating that the substantial agreement between the results of XANES and EXAFS analyses was obtained. Therefore, it is concluded that the deconvolution analysis of Ga K-edge XANES can be used to estimate the relative ratio of the Ga species with tetrahedral and octahedral symmetries in gallium oxide samples. Generally, the intensity of XANES spectra is higher than the intensity of EXAFS oscillation. In addition, the data analysis of the present method is much simpler than the curve-fitting analysis of EXAFS. Therefore, the deconvolution analysis of XANES is considered to be a novel characterization method for studying the local structure of gallium oxide compounds. The relationship between the local structure and the alkane dehydrogenation activity of the above-characterized gallium oxide catalysts is under investigation and will be reported elsewhere.[30]

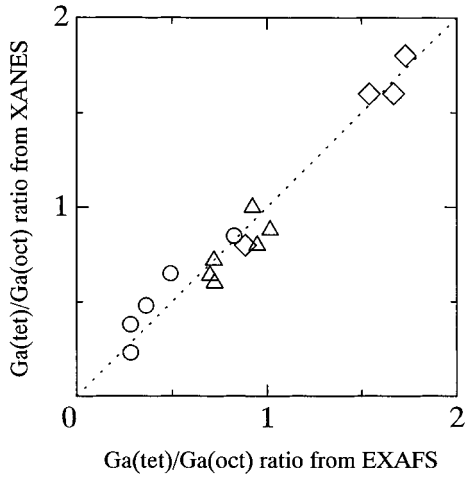

Figure 5. Plot of Ga(t)/Ga(o) ratio derived from the deconvolution analysis of XANES versus that from curve-fitting analysis of EXAFS. Samples are prepared (○) from hydroxide (H-*n*) and (△) from nitrate (N-*n*) and (◇) supported on SiO_2 (S-*n*).

Conclusion

X-ray absorption spectroscopy (XANES and EXAFS) of Ga K-edge was recorded on a series of gallium oxides with variety of crystal phases, crystallinity, and dispersion states. XANES spectra showed two distinguishable peaks due to tetrahedral and octahedral Ga species. Deconvolution analysis of XANES could

quantitatively provide an estimate of the ratio of those species, which was confirmed by the EXAFS curve-fitting analysis. Deconvolution analysis of XANES is provided as a novel characterization method for the quantitative analysis of Ga coordination states (tetrahedral and octahedral) in gallium oxides.

Acknowledgment. The X-ray absorption experiment was performed under the approval of the Photon Factory Program Advisory Committee (Proposal No. 96G-002). The authors thank Mr. Shin-ich Komai of Nagoya University for his technical assistance. H.Y. thanks Dr. Patrick Berthet of Universite Paris Sud for his kindness.

References and Notes

(1) Ono, Y. *Catal. Rev. Sci. Eng.* **1992**, *34*, 179.
(2) Guisnet, M.; Gnep, N. S.; Alario, F. *Appl. Catal.* **1992**, *89*, 1.
(3) Thomas, J. M.; Liu, X.-S. *J. Phys. Chem.* **1986**, *90*, 4843.
(4) Corberan, V. C.; Valenzuela, R. X.; Sulikowski, B.; Derewinski, M.; Olejniczak, Z.; Krysciak, J. *Catal. Today* **1996**, *32*, 193.
(5) Roy, R.; Hill, V. G.; Osborn, E. F. *J. Am. Chem. Soc.* **1952**, *74*, 719.
(6) Morterra, C.; Magnacca, G. *Catal. Today* **1996**, *27*, 497.
(7) Geller, S. *J. Chem. Phys.* **1960**, *33*, 676. (Ga(t) is surrounded by a distorted tetrahedron of oxygen atoms with Ga−O = 1.80−1.85 Å, while Ga(o) is surrounded by a distorted octahedron of oxygen atoms with Ga−O = 1.95−2.08 Å.)
(8) Marezio, M.; Remeika, J. P. *J. Chem. Phys.* **1967**, *46*, 1862.
(9) Coster, D.; Blumenfeld, A. L.; Fripiat, J. *J. Phys. Chem.* **1994**, *98*, 6201.
(10) K.-Fandrei, G.; Bastow, T. J.; Hall, J. S.; Jager, C.; Smith, M. E. *J. Phys. Chem.* **1995**, *99*, 15138.
(11) Timken, H. K. C.; Oldfield, E. *J. Am. Chem. Soc.* **1987**, *109*, 7669.
(12) Bayense, C. R.; van Hooff, J. H. C.; Kentgens, A. P. M.; de Haan, J. W.; van de Ven, L. J. M *J. Chem. Soc., Chem. Commun.* **1989**, 1292.
(13) Bayense, C. R.; Kentgens, A. P. M.; de Haan, J. W.; van de Ven, L. J. M.; van Hooff, J. H. C. *J. Phys. Chem.* **1992**, *96*, 775.
(14) Sulikowski, B.; Olejniczak, Z.; Corberán, V. C. *J. Phys. Chem.* **1996**, *100*, 10323.
(15) Bart, J. C. J. *Adv. Catal.* **1986**, *34*, 203.
(16) Iwasawa, Y., Ed. *X-ray Absorption Fine Structure for Catalysts and Surfaces*; World Scientific: Singapore, 1996; Chapter 8.
(17) Shimizu, K.; Takamatsu, M.; Nishi, K.; Yoshida, H.; Satsuma, A.; Hattori, T. *Chem. Commun*. **1996**, 1827.
(18) Murakami, Y. *Stud. Surf. Sci. Catal.* **1983**, *16*, 775.
(19) Nomura, M.; Koyama, A. KEK Report 89-16, 1989.
(20) Tanaka, T.; Yamashita, H.; Tsuchitani, R.; Funabiki, T.; Yoshida, S. *J. Chem. Soc., Faraday Trans. 1* **1988**, *84*, 2987.
(21) Dymock, K.; Palenik, G. J. *Acta Crystallogr. B* **1974**, *30*, 1364.
(22) Tourtin, F.; Armand, P.; Ibanez, A.; Tourillon, G.; Philippot, E. *J. Phys. (France)* **1997**, *7*, C2-975.
(23) Stave, M. S.; Nicholas, J. B. *J. Phys. Chem.* **1995**, *99*, 15046.
(24) Wong, J.; Rek, Z. U.; Rowen, M.; Tanaka, T.; Schäfers, F.; Müller, B.; George, G. N.; Pickering, I. J.; Via, G.; DeVries, B.; J. Brown, G. E.; Fröba, M. *Physica B* **1995**, *208−209*, 220.
(25) Cramer, S. P.; Eccles, T. K.; Kutzler, F. W.; Hondgson, K. O.; Mortenson, L. E. *J. Am. Chem. Soc.* **1976**, *98*, 1287.
(26) Vlaic, G.; Bart, J. C. J.; Cavigiolo, W.; Mobilio, S. *Chem. Phys. Lett.* **1980**, *15*, 453.
(27) Brown, N. M. D.; McMonagle, J. B.; Greaves, G. N. *J. Chem. Soc., Faraday Trans. 1* **1984**, *80*, 589.
(28) Wong, J.; Lytle, F. W.; Messmer, R. P.; Maylotte, D. H. *Phys. Rev. B* **1984**, *30*, 5596.
(29) Tanaka, T.; Hanada, T.; Yoshida, S.; Baba, T.; Ono, Y. *Jpn. J. Appl. Phys.* **1993**, *32* (2), 481.
(30) Nishi, K.; Takamatsu, M.; Shimizu, K.; Yoshida, H.; Satsuma, A.; Hattori, T. Manuscript in preparation.